Design of Three-winding Coupled Inductor for Minimum Current Ripple in Battery Chargers

Taewon Kang and Yongsug Suh
Dept. of Electrical Engineering, Smart Grid Research Center, Chonbuk National University

Abstract

This paper investigates the design of coupled inductor for minimum inductor current ripple in rapid traction battery charger systems. Based on the general circuit model of coupled inductor together with the operating principles of dc-dc converter, the relationship between the ripple size of inductor current and the coupling factor is derived under the different duty ratio. The optimal coupling factor which corresponds to a minimum inductor ripple current becomes -0.5, i.e. a complete inverse coupling without leakage inductance, as the steady-state duty ratio operating point approaches 1/3 or 2/3. In an opposite manner, the optimal coupling factor value of zero, i.e. zero mutual inductance, is required when the steady-state duty ratio operating point approaches either zero or one. Coupled inductors having optimal coupling factor can minimize the ripple current of inductor and battery current resulting in a reliable and efficient operation of battery chargers.

1. Introduction

Plug-in Hybrid Electric Vehicle (PHEV) is becoming an attractive alternative to internal combustion engine vehicles in modern transportation industry. One way to achieve the practical all-electric cruising range of electric vehicles is to implement well distributed fast charger infrastructure. Therefore, battery chargers play a critical role in the development of EVs. EV battery chargers can be classified into on-board and off-board with unidirectional or bidirectional power flow. Unlike on-board chargers, off-board battery chargers are less constrained by size and weight. In contrary, charging time and battery life are closely linked to the characteristics of the off-board battery charger. Various topologies and schemes have been reported for off-board chargers [1-3].

Among several topologies for off-board chargers, parallel connected multiple bidirectional dc-dc converters with active or diode bridge front-end rectifier are well adopted in industry. Phase-staggering operation of multiple bidirectional dc-dc converters is considered to reduce the ripple size of summed inductor currents and filtering requirement for the battery charging current. Reduction of inductor current ripple by a coupled inductor in the interleaving structure has been also proposed. A coupled inductor can further decrease the physical size of inductor itself while still complying with the peak switching current requirements from power semiconductor switches in dc-dc converters [4-6]. In [4], analysis on coupled inductor along with core design for boost converter has been presented. The operating principle of coupled inductor in an interleaved buck converter has been investigated in [5]. Design of multi-winding coupled inductor has been reported in [6]. The coupling factor of coupled inductor has a significant impact on the phase-staggering operation of multiple bidirectional dc-dc converters. The selection of the optimal magnetic structure and coupling factor is regarded to be an important task in designing a coupled inductor. However, there has been a little work focusing on the optimal coupling factor of a coupled inductor and its relationship with the operation of dc-dc converters in previous literatures.

This paper investigates the design of 3-winding coupled inductor for minimum inductor current ripple in rapid traction battery charger systems. The influence of coupling factor of 3-winding coupled inductor on the operation of interleaved dc-dc converters is studied. The selection of optimal coupling factor under various operating conditions is also presented.

2. Modeling of Coupled Inductor

Figure 1 shows the schematic of rapid charger system considered in this paper. Overall battery charging and discharging system consists of active front-end rectifier of neutral point clamped 3-level type and non-isolated bidirectional dc-dc converter of multi-phase interleaved half-bridge topology.

The large ripple in battery charging current incurs stresses to a battery and eventually shortens the life time of battery. In order to reduce the ripple of battery charging current and the size of filter inductor, coupling of output inductors in three-phase interleaved dc-dc converters is employed. Interleaved bi-directional dc-dc converter with the 3-widing coupled inductor core structure is shown in Fig. 3. The coupled inductor has the symmetric magnetic structure having three legged core. The equivalent circuit of 3-winding coupled inductor is illustrated in Fig. 4. Equivalent circuit of 3-winding coupled inductor is based on transformer equivalent circuit. This circuit basically consists of three leakage inductances and one mutual inductance. The core structure has three legs of Y-

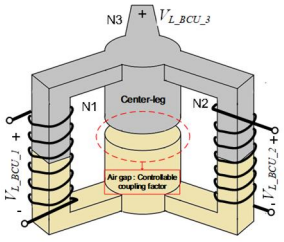

Fig 3 Magnetic structure of 3-winding coupled inductor

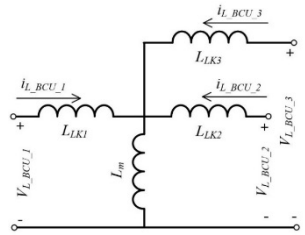

Fig 4 Equivalent circuit of 3-winding coupled inductor

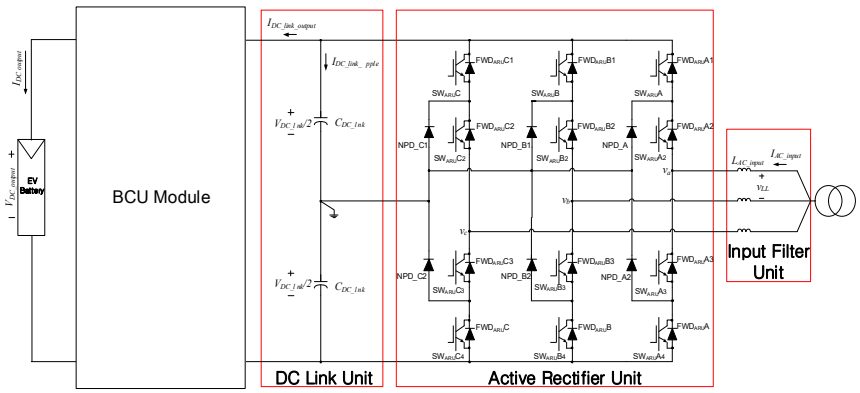

Fig 1 Battery charging and discharging inverter system

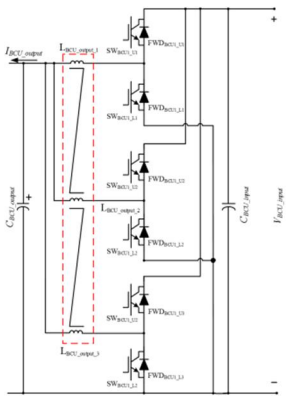

Fig 2 Bi-directional DC-DC converter

Y core so that the coupling factor among three windings can be adjusted by the air gap distance in the center leg.

3. Design of Optimized Coupling Factor

Among many design factors related with a coupled inductor, the coupling factor between multiple windings plays an important role in determining various characteristics of coupled inductor such as a ripple size of inductor current. It is of high practical importance to find an optimized coupling factor which generates the least ripple size of inductor current under different operating conditions. Optimized coupling factor for the minimum inductor current ripple is derived based on the equivalent circuit of coupled inductor in Fig. 4 and the phase-staggering operation of three paralleled buck converters in Fig. 2.

$$V_{L\_BCU\_1} = \frac{d}{dt}(\lambda_{11} + \lambda_{21} + \lambda_{31}) = L_{11}\frac{d}{dt}i_{L\_BCU\_1} + L_{21}\frac{d}{dt}i_{L\_BCU\_2} + L_{31}\frac{d}{dt}i_{L\_BCU\_3} \quad (1)$$

$$V_{L\_BCU\_2} = \frac{d}{dt}(\lambda_{22} + \lambda_{12} + \lambda_{32}) = L_{22}\frac{d}{dt}i_{L\_BCU\_2} + L_{12}\frac{d}{dt}i_{L\_BCU\_1} + L_{32}\frac{d}{dt}i_{L\_BCU\_3} \quad (2)$$

$$V_{L\_BCU\_3} = \frac{d}{dt}(\lambda_{33} + \lambda_{13} + \lambda_{23}) = L_{33}\frac{d}{dt}i_{L\_BCU\_3} + L_{13}\frac{d}{dt}i_{L\_BCU\_1} + L_{23}\frac{d}{dt}i_{L\_BCU\_2} \quad (3)$$

$$k = \frac{M}{\sqrt{L_{11}L_{22}}} = \frac{M}{\sqrt{L_{11}L_{33}}} = \frac{M}{\sqrt{L_{22}L_{33}}} \quad (4)$$

$$(k+1)V_{L\_BCU\_1} - kV_{L\_BCU\_2} - kV_{L\_BCU\_3} = (1 + k - 2k^2)L_{11}\frac{d}{dt}i_{L\_BCU\_1} \quad (5)$$

$$V_{L\_BCU\_1} = L_{eq}\frac{d}{dt}i_{L\_BCU\_1}, V_{L\_BCU\_2} = L_{eq}\frac{d}{dt}i_{L\_BCU\_2}, V_{L\_BCU\_3} = L_{eq}\frac{d}{dt}i_{L\_BCU\_3} \quad (6)$$

In (7)-(9), the total peak-to-peak ripple size of inductor current under the condition of $0 < D < 1$.

$$\Delta i_{L\_pp\_total\_0<D<1/3} = \Delta i_{L\_pp\_m1} = \frac{V_{in} - V_o}{L_{eq\_m1}}DT \quad (7)$$

$$\Delta i_{L\_pp\_total\_1/3<D<2/3} = \Delta i_{L\_pp\_m5} + \Delta i_{L\_pp\_m6} + \Delta i_{L\_pp\_m1} = \left(\frac{V_{in} - V_o}{L_{eq\_m5}} + \frac{V_{in} - V_o}{L_{eq\_m6}}\right)\left(D - \frac{1}{3}\right)T + \frac{V_{in} - V_o}{L_{eq\_m1}}\left(\frac{2}{3} - D\right)T \quad (8)$$

$$\Delta i_{L\_pp\_total\_2/3<D<1} = \Delta i_{L\_pp\_m7} = \frac{V_o}{L_{eq\_m7}}(1 - D)T \quad (9)$$

$$\Delta i_{L\_pp\_total\_0<D<1/3} = \frac{V_{in}DT}{L_s}\frac{(1-D)\left(1 + k + 2k\frac{D}{(1-D)}\right)}{1 + k - 2k^2} \quad (10)$$

$$\Delta i_{L\_pp\_total\_1/3<D<2/3} = \frac{V_{in}(1-D)T}{L_s}\frac{\left(D - Dk + \frac{2}{3}k + \frac{2D}{3(1-D)}k\right)}{1 + k - 2k^2} \quad (11)$$

$$\Delta i_{L\_pp\_total\_2/3<D<1} = \frac{V_{in}DT}{L_s}\frac{(1-D)\left(1 + k + 2k\frac{(1-D)}{D}\right)}{1 + k - 2k^2} \quad (12)$$

The optimal coupling factors maximizing the corresponding equivalent inductance values of (10), (11), and (12) under three different regions of duty ratio are derived and expressed in (13), (14), and (15), respectively.

$$k_{opt\_\ 0<D<1/3} = -\frac{1 - D - \sqrt{1 - 3D}}{D + 1} \quad (13)$$

$$k_{opt\_\ 1/3\ <\ D\ <\ 2/3} = -\frac{D - D^2 - \sqrt{-D^2 + D - \frac{2}{9}}}{D^2 - D + \frac{2}{3}} \quad (14)$$

$$k_{opt\_\ 2/3\ <\ D\ <\ 1} = -\frac{(D - D^2) - \sqrt{3D^3 - 8D^2 + 7D - 2}}{D^2 - 3D + 2} \quad (15)$$

TABLE I
EQUIVALENT INDUCTANCE UNDER DIFFERENT SWITCH MODE

Mode	SW Condition	Equivalent inductance (L_{eq})	Mode	SW condition	Equivalent inductance (L_{eq})
Mode 1	$SW_{BCU_{U1}}$ = On $SW_{BCU_{U2}}$ = Off $SW_{BCU_{U3}}$ = Off	$L_{eq} = \frac{1 + k - 2k^2}{1 + k + 2\frac{D}{1-D}k}L_{11}$	Mode 5	$SW_{BCU_{U1}}$ = On $SW_{BCU_{U2}}$ = Off $SW_{BCU_{U3}}$ = On	$L_{eq} = \frac{1 + k - 2k^2}{1 + \frac{D}{1-D}k}L_{11}$
Mode 2	$SW_{BCU_{U1}}$ = Off $SW_{BCU_{U2}}$ = Off $SW_{BCU_{U3}}$ = Off	$L_{eq} = \frac{1 + k - 2k^2}{1 - k}L_{11}$	Mode 6	$SW_{BCU_{U1}}$ = On $SW_{BCU_{U2}}$ = On $SW_{BCU_{U3}}$ = Off	$L_{eq} = \frac{1 + k - 2k^2}{1 + \frac{D}{1-D}k}L_{11}$
Mode 3	$SW_{BCU_{U1}}$ = Off $SW_{BCU_{U2}}$ = On $SW_{BCU_{U3}}$ = Off	$L_{eq} = \frac{1 + k - 2k^2}{1 + \frac{1-D}{D}k}L_{11}$	Mode 7	$SW_{BCU_{U1}}$ = Off $SW_{BCU_{U2}}$ = On $SW_{BCU_{U3}}$ = On	$L_{eq} = \frac{1 + k - 2k^2}{1 + k + 2\frac{1-D}{D}k}L_{11}$
Mode 4	$SW_{BCU_{U1}}$ = Off $SW_{BCU_{U2}}$ = Off $SW_{BCU_{U3}}$ = On	$L_{eq} = \frac{1 + k - 2k^2}{1 + \frac{1-D}{D}k}L_{11}$	Mode 8	$SW_{BCU_{U1}}$ = On $SW_{BCU_{U2}}$ = On $SW_{BCU_{U3}}$ = On	$L_{eq} = \frac{1 + k - 2k^2}{1 - k}L_{11}$

4. System Verification

TABLE II. SPECIFICATIONS OF ELECTRIC VEHICLE BATTERY CHARGE SYSTEM

Specification	Values	Specification	Values
Rated power	30kW	AC input voltage	342~506V
AC input current	77A	DC-link voltage	858V
DC output voltage	50~450V	Battery capacity	11 4kWh
CV mode voltage	440	CC mode current	78A

This work was supported by the National Research Foundation of Korea(NRF) grant funded by the Korea government (MSIP) (No 2010-0028509) & (No 2014R1A2A1A11053678)

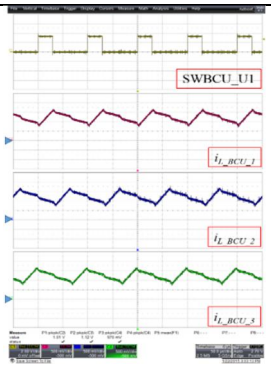

Fig 5 Experiment waveforms of coupled inductor current under duty = 0 3 and coupling factor = -0 295 ($i_{L\_BCU\_1}$, $i_{L\_BCU\_2}$, $i_{L\_BCU\_3}$ [10A/div, 50us/div])

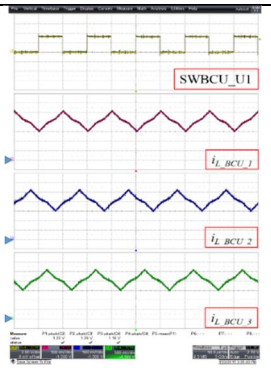

Fig 6 Experiment waveforms of coupled inductor current under duty = 0 5 and coupling factor = -0 2 ($i_{L\_BCU\_1}$, $i_{L\_BCU\_2}$, $i_{L\_BCU\_3}$ [10A/div, 50us/div])

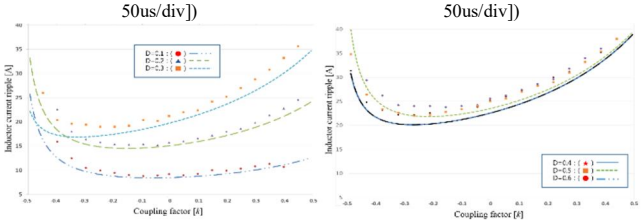

Fig 7 Mathematical and experimental data of inductor current ripple vs coupling factor under $0 < D < 1/3$ and $1/3 < D < 2/3$ [line : mathematical analysis, dot : experiment]

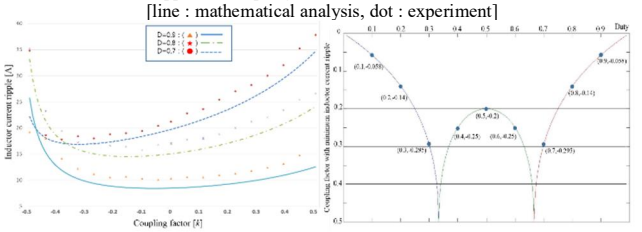

Fig 8 Mathematical and experimental data of inductor current ripple vs coupling factor under $2/3 < D < 1$ [line : mathematical analysis, dot : experiment]

Fig 9 3-winding coupling factor of the minimum inductor current ripple vs duty [line : mathematical analysis, dot : experiment]

5. Conclusion

Coupled inductors are often employed in several topologies for battery charger systems. Through an appropriate coupling factor and phase-staggering operation, coupled inductor can improve the performance of charging unit with smaller inductor ripple current. This paper investigates the design of 3-winding coupled inductor for minimum inductor current ripple in rapid traction battery charger systems. Based on the general circuit model of 3-winding coupled inductor together with the operating principles of dc-dc converter, the relationship between the ripple size of inductor current and the coupling factor is derived. The optimal coupling factor which corresponds to a minimum inductor ripple current becomes -0.5, i.e. a complete inverse coupling without leakage inductance, as the steady-state duty ratio operating point approaches 1/3 or 2/3.

Experimental result verify the theoretical derivation of the optimal coupling factor. The design guideline for selecting optimal coupling factor can be very useful in designing of a battery charging system. Coupled inductors having optimal coupling factor can minimize the ripple current of inductor and also the battery ripple current resulting in a reliable and efficient operation of battery chargers.

References

[1] M. Bojrup, P. Karlsson, M. Alakula, and B. Simonsson, "A dual purpose battery charger for electric vehicles," in *IEEE Power Electronics Specialists Conference*, vol. 1, pp. 565-570, 1998.
[2] C.C. Chan and K.T. Chau, "An overview of power electronics in electric vehicles," in *IEEE Trans. Ind. Appl.*,vol.44,no. 1, pp. 3-13, Feb. 1997.
[3] Murat Yilmaz, Philop T. Krein, "Review of battery charger topology, charging power levels, and infrastructure for plug-in electric and hybrid vehicles," in *IEEE Transactions on Power Electronics*, vol. 28, no.5, pp.2151-2169, 2013.
[4] Jun Imaoka and Masayoshi Yamamoto, "A novel integrated magnetic structure suitable for transformer-linked interleaved boost chopper circuit" in *Energy Conversion Congress and Exposition (ECCE) 2012 IEEE*, pp.3279-3284, 2012.
[5] Pit-Leong and Wong, Peng Xu "Performance improvements of interleaving VRMs with coupled inductors" in *IEEE Transactions on Power Electronics*, vol.16, no.4, 2011.
[6] *Nagaraja H.N "Design principles of a symmetrically coupled inductor strucutre for multiphase synchronous buck converters" in IEEE Transactions on Power Electronics vol.58 no.3 2011.*
[7] *J. Czogalla J. Li and C.R. Sullivan "Automotive Application of Multi-Phase Coupled-Inductor DC-DC Converter " in IEEE Industry Applications Conference vol. 3 pp. 1524-1529 2003.*